



Korablev, O., Vandaele, A. C. (2019). No detection of methane on Mars from early ExoMars Trace Gas Orbiter observations. *Nature*, 568, 517-520. <https://doi.org/10.1038/s41586-019-1096-4>

Peer reviewed version

Link to published version (if available):
[10.1038/s41586-019-1096-4](https://doi.org/10.1038/s41586-019-1096-4)

[Link to publication record in Explore Bristol Research](#)
PDF-document

This is the accepted author manuscript (AAM). The final published version (version of record) is available online via Nature at <https://doi.org/10.1038/s41586-019-1096-4> . Please refer to any applicable terms of use of the publisher.

University of Bristol - Explore Bristol Research

General rights

This document is made available in accordance with publisher policies. Please cite only the published version using the reference above. Full terms of use are available:
<http://www.bristol.ac.uk/red/research-policy/pure/user-guides/ebr-terms/>

Early observations by ExoMars Trace Gas Orbiter show no signs of methane on Mars

Oleg Korablev¹, Ann Carine Vandaele², Franck Montmessin³, Anna Fedorova¹, Alexander Trokhimovskiy¹, Francois Forget⁴, Franck Lefèvre³, Frank Daerden², Loïc Trompet², Justin Erwin², Shohei Aoki², Séverine Robert², Ian R. Thomas², Sébastien Viscardy², Alexey Grigoriev¹, Nikolay Ignatiev¹, Alexey Shakun¹, Andrey Patrakeev¹, Denis Belyaev¹, Jean-Loup Bertaux^{1,3}, Kevin S. Olsen³, Lucio Baggio³, Juan Aulday⁴, Bojan Ristic², Manish R. Patel⁵, Giancarlo Bellucci⁶, Jose-Juan Lopez-Moreno⁷, Colin F. Wilson⁸, Giuseppe Etiope⁹, Lev Zelenyi¹, Håkan Svedhem¹⁰, Jorge L. Vago¹⁰,

and the ACS and NOMAD Teams

1 Space Research Institute (IKI) Moscow, Russia

2 Royal Belgian Institute of Space Aeronomy BIRA-IASB, Brussels, Belgium

3 LATMOS, UVSQ Université Paris-Saclay, Sorbonne Université, CNRS, France

4 LMD CNRS Jussieu, Paris, France

5 Open University, Milton-Keynes, UK

6 IAPS-INAF, Rome, Italy

7 Instituto de Astrofísica de Andalucía/CSIC, Granada, Spain

8 Physics Department, Oxford University, Oxford, UK

9 Istituto Nazionale di Geofisica e Vulcanologia, Rome, Italy; Faculty of Environmental Science and Engineering, Babes-Bolyai University, Cluj-Napoca, Romania.

10 ESA-ESTEC, Noordwijk, the Netherlands

The detection of methane on Mars has been interpreted as indicating that geochemical or biological activities could persist on Mars today. A few plumes with concentration levels of 7-45 parts per billion (ppbv) and lasting for a few weeks have been reported from both remote sensing¹ and from *in situ* measurements². Outside of these events, the Curiosity rover measured a background level of methane of 0.41 ± 0.16 ppbv at the surface, varying with season⁶. As the theoretical lifetime of methane is centuries long, it should be evenly mixed by atmospheric circulation⁷. Therefore the fast transition from high-concentration “plumes” to the “background” values 10–30 times lower, and the observed seasonal cycle of the background levels, are both scientifically puzzling^{7,6}. Here we report results that, when confronted with those of Curiosity, make methane presence on Mars even more enigmatic. These results were obtained from sensitive atmospheric soundings by the ACS and NOMAD instruments onboard the ESA-Roscosmos ExoMars Trace Gas Orbiter (TGO). Using these two independent instruments observing daily over

a few months before and during the 2018 global dust storm over a wide range of latitudes in both hemispheres, we could not detect any signature of methane. We, therefore, establish a new upper limit for methane abundance of ~ 0.05 ppbv, ten times lower than the background level measured by Curiosity at the same season⁶. No known mechanism can explain this discrepancy. Reconciling the TGO measurements with methane concentrations reported in the past, in particular, those of Curiosity, requires that an unknown process quickly eradicates methane while it resides in the first kilometres of the martian boundary layer.

The first positive detections of methane on Mars were published in 2004 from the analysis of 1999 ground-based spectroscopic observations³, and from the Planetary Fourier Spectrometer (PFS) instrument on board ESA's Mars Express orbiter⁸. Mixing ratios of methane of ~ 10 ppbv were reported. This stirred up excitement in the scientific community but both observations were at the limit of sensitivity. In 2003, new ground-based echelle-spectroscopy observations reported a plume of methane developed over 60 northern summer sols¹, and reaching a peak value of 45 ± 10 ppbv. No methane ($\leq 7-8$ ppbv) was detected before and after the event^{1, 4, 5}. Starting from 2012 the Tunable Laser Spectrometer (TLS) of the Sample Analysis at Mars (SAM) instrument onboard NASA's Curiosity rover performed local samplings of Mars' atmosphere in Gale crater. A release of 10 ppbv was detected in 2012, followed by a few isolated ~ 6 ppbv readings, the most recent in 2017. All other measurements to date have remained below ~ 2 ppbv. More sensitive TLS samplings led to the discovery of a seasonally varying "background level" ranging between 0.24 and 0.65 ppbv⁶.

In the oxidizing Mars atmosphere methane is slowly destroyed by UV photolysis and reactions with OH and O(¹D). Based on our current understanding of Mars photochemistry, it should have a lifetime of 250-300 years^{7,18}. Therefore, its detection, even in small quantities, requires a sustained replenishment. This has attracted much interest because on Earth, most of the atmospheric methane has a biological origin. Thus the Martian atmospheric methane might hint at active or extant microbial life or at the existence of organic matter. However, methane can also be formed abiotically, by low-temperature chemical reactions (e.g., CO₂ hydrogenation) or magmatic processes^{19,20}.

Given its potential implications for exobiology or geochemistry, highly sensitive measurements of atmospheric methane and other trace species were identified as the primary science goal of the TGO mission^{10,11}. The 2-hour circular orbit of the TGO satellite was designed for detecting trace gases using solar occultations, a technique in which the spacecraft instruments observe the atmospheric absorption spectrum of sunlight during sunsets and sunrises¹². Solar occultations provide very high sensitivity for trace gas concentration measurements because: (1) the Sun's brightness results in

very high signal to noise ratio (SNR) spectra; and (2) the atmospheric optical path length in occultation viewing geometry is $\sim 30\times$ longer than that achieved when observing the planet's surface. Two instrument suites on board TGO were designed to perform such measurements: ACS (the Atmospheric Chemistry Suite)¹³ and NOMAD (Nadir and Occultation for Mars Discovery)¹⁴. Both ACS and NOMAD cover the $3.3\ \mu\text{m}$ spectral range that includes the strongest fundamental absorption bands for hydrocarbons such as CH_4 , in particular, the ν_3 asymmetric stretching band on which all the previous detections were made. TGO started its science operations in April 2018, with the first occultation taking place on April 21st. Before the 2018 planetary encircling dust storm reduced the transparency of the atmosphere (see companion paper¹⁵), the most sensitive channels of ACS and NOMAD performed 32 (ACS) and 292 (NOMAD) occultation observations in the CH_4 range (Figure 1).

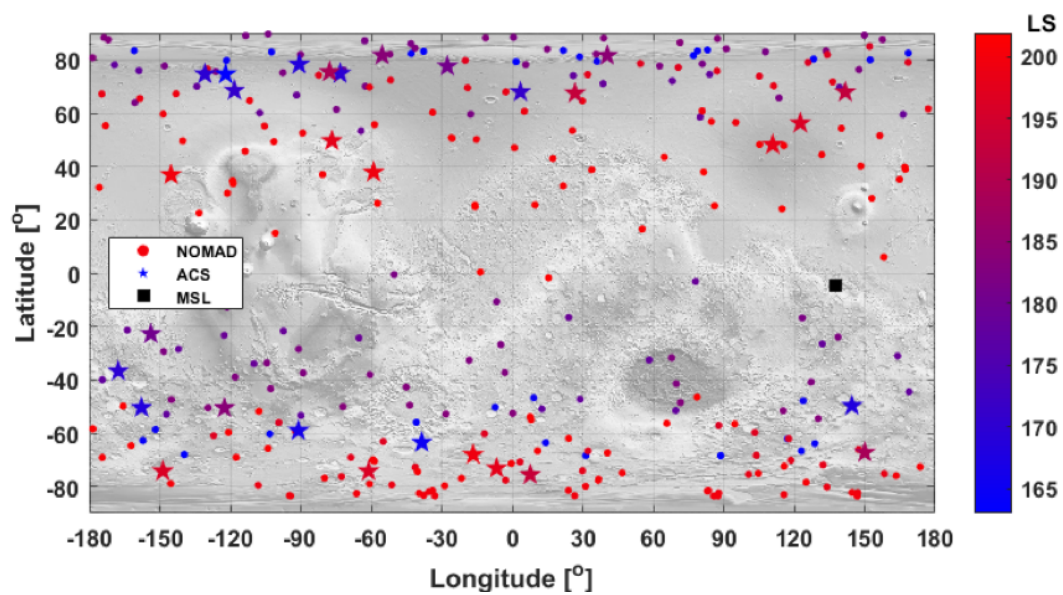


Figure 1. The map of ExoMars TGO methane measurements by ACS (stars) and NOMAD (circles) obtained between April 21 and June 29, 2018. The colour scale denotes L_s (the areocentric solar longitude). Gale crater (the Curiosity rover location) is marked by a bold, black square.

When staring at the solar disk outside the atmosphere, the SNR for ACS MIR (mid-IR) channel reaches 10,000 (one detector line, 2 s integration time, 2.5 km vertical sampling rate), and for NOMAD Solar Occultation (SO) channel ~ 2000 (one spectrum, 48 ms integration time, 1 km sampling rate). During a solar occultation, the trace gas detection sensitivity increases as the line of sight progressively samples closer to the surface, thereby intersecting a larger volume of atmosphere. However, the measurements' sensitivity suffers from the presence of dust and clouds, which can drastically reduce the intensity of light reaching the instrument. The optimum sensitivity is thus achieved at the lowest altitude where the atmosphere is transparent enough. Typically, this corresponds to the level for which atmospheric transmission is 0.2–0.4. Figure 2 shows examples of spectra acquired at an altitude close to the optimal one. No methane absorptions are apparent,

while we accurately measure the faint H₂O lines within the range, which, at very low water content, have an absorption depth comparable to a 1 ppbv CH₄ absorption.

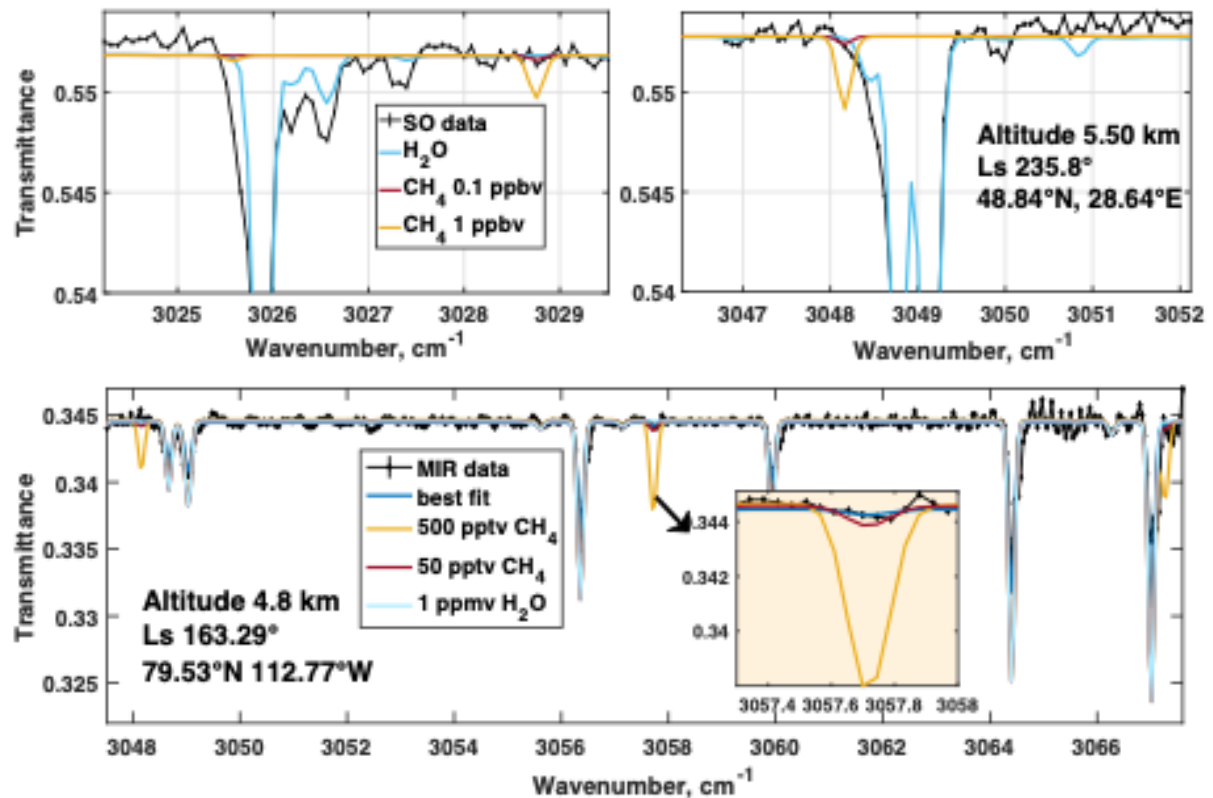


Figure 2. Panel A: Example of spectra obtained by NOMAD SO (spectra binned to the equivalent 3.5 s integration time, 25 km sampling rate) in two different diffraction orders corresponding to the R-branch of the CH₄ band. The measured spectra are plotted together with synthetic spectra assuming 1 ppbv and 0.1 ppbv of CH₄ or the water vapour absorption. Panel B: similar results obtained by ACS MIR (2 s integration time, 2.5 km sampling rate) before the dust storm in much cleaner and drier (≤ 1 ppmv of H₂O) conditions. The spectrum range of one ACS diffraction order includes the same methane feature of methane as in Panel A (3048.2 cm⁻¹), and two stronger isolated features, allowing to constrain the methane content below tens of pptv.

Retrieved profiles of H₂O (see Methods), obtained in very dry conditions, are characterized by an unprecedented accuracy compared to previous profiling¹⁶ (see companion paper¹⁵). The effect of the atmospheric aerosol loading on the retrieval accuracy was previously discussed¹³. Based on the noise level, CH₄ absorption, integrated over the line of sight, can be tentatively fitted along with absorption of CO₂ while taking into account instrument spectral resolution (see Methods). This way, an estimation of methane detection limits, converted into volume mixing ratios, for the full data set acquired by ACS and NOMAD was made. Figure 3 illustrates the detection limits for the ensemble of observations performed by both instruments. On average, the best levels of detection are achieved

between 15 and 25 km¹³. A few profiles, measured in cleaner northern conditions, were able to achieve the most precise detection limits of 0.012 ppbv down to an altitude of ~3 km (cf. Figure 3).

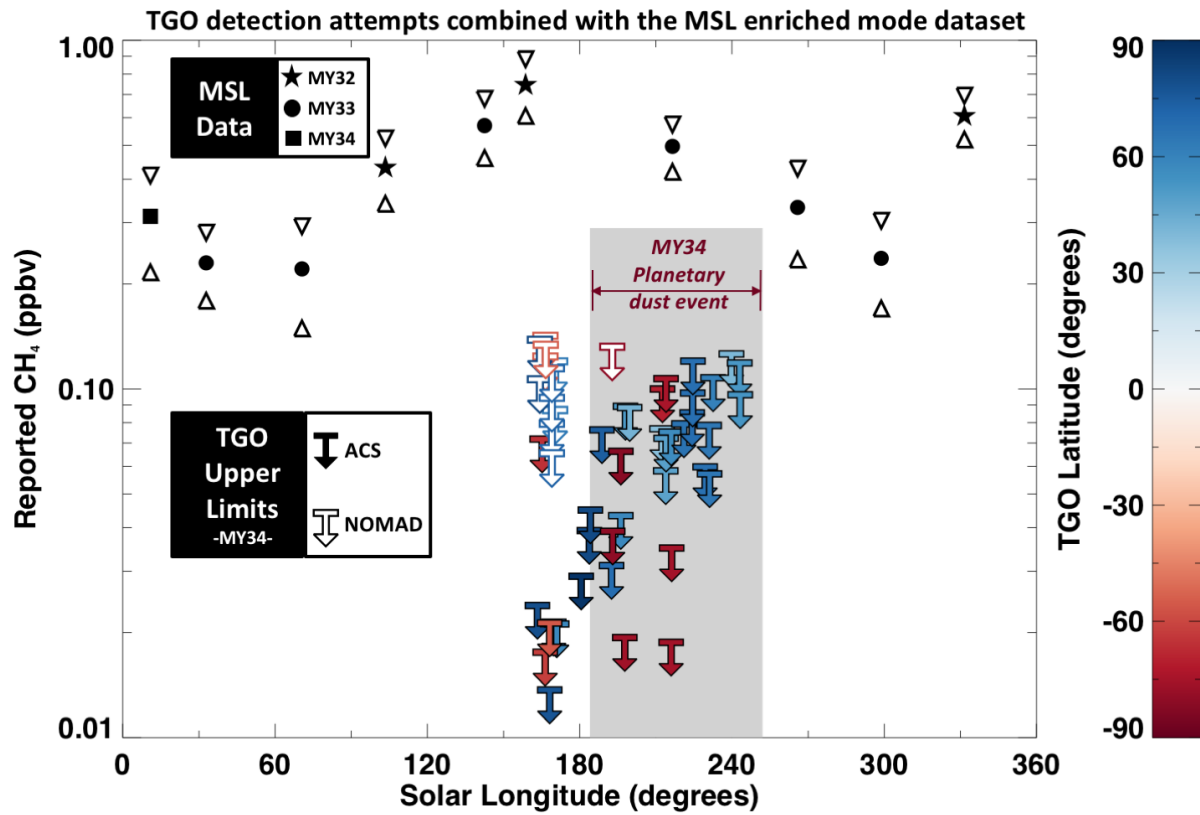


Figure 3. Upper limits for CH₄ obtained by TGO (ACS and NOMAD) compared to seasonally variable background methane as measured by SAM-TLS on Curiosity. The colour scale gives the latitude of TGO sampling. Both ACS and NOMAD datasets have been filtered to retain only the most precise upper limits which are most relevant for the sake of comparing them with MSL results. For this reason, only retrieved upper limits found below a threshold of 0.15 ppbv are displayed, encompassing values down to 0.012 ppbv. The gradual increase in upper limits observed after the onset of the Planetary dust event (shown in light grey) is a direct consequence of dust forcing detections to occur progressively above 30 km, that is above the theoretically optimal altitude (detection-wise) usually found between 15 to 25 km.

This non-detection of methane by TGO and its associated upper limits are in contradiction with the 0.5 ppbv background levels measured *in situ* by Curiosity at the same season⁶ in previous years. As discussed above, TGO is able to detect concentrations at least ten times lower than 0.5 ppbv. In fact, a simple comparison of the theoretical sensitivity of the solar occultation method with the TLS instrument method shows that TGO should be more sensitive than what can be achieved

with the TLS, even when the measurements are performed using the TLS enrichment mode (see Methods).

Is it possible that the factor of ten difference between the MSL measurements and the TGO upper limits could result from spatial variations in the methane mixing ratios? MSL measurements were obtained at the bottom of Gale Crater near the equator, while the best TGO measurements were achieved in the near-polar latitudes and a few kilometres above the surface. However, It is difficult to understand why the martian atmosphere would permit such a spatial differentiation of concentrations. On Mars, the daytime atmospheric boundary layer is characterized by intense convective motions, which mix any trace gas such as methane efficiently on a daily basis from the surface up to the top of the convective boundary layer, usually 6 to 10 kilometres high. From there the global wind circulation transports trace gases horizontally^{7,27} and vertically around the planet. Global uniform mixing of methane occurs on a scale of 2 to 3 months^{7,28}. Even in the unlikely case where Gale Crater would constitute the sole source of methane on Mars (note that Gale Crater and surrounding areas along the martian dichotomy host geological features where methane could be released²⁰), MSL measurements still remain in disagreement with the detection limits derived from TGO measurements. Indeed, if we assume that Gale is uniformly and constantly filled with 0.5 ppbv of CH₄ up to its lowest rim (at ~2 km) and that a mixing timescale of 1 sol⁶ is the typical time for air to leave the crater, Gale emission would lead CH₄ to accumulate globally over one year at a level of ~2 pptv. This implies that such a background emission from Gale crater could only have been going on for at most 20 years before the detection limits reported here would have been reached. Taking into account the ppbv spikes of CH₄ concentration reported by MSL, this time would be even more reduced. To maintain a level of methane ten times higher than elsewhere, Gale Crater should not only be the unique source, it should also preserve its air mass from exchanging with the global atmosphere. Interestingly, mesoscale model simulations have shown that the depth of the boundary layer in Gale crater is significantly lowered³⁰ due to the crater size and depth. Even if this would tend to maintain methane locally, the same simulation^{30, 31} shows that the slope winds on the side of the crater and the induced updraft above the rims is so intense that methane should be efficiently injected into the atmosphere at 10 km altitude. In any case can we consider Gale to be an isolated crater.

To reconcile the absence of methane in the TGO data and the positive methane detection at the surface by Curiosity, one must invoke a mechanism able to fully eradicate methane in the lower atmosphere at a rate ~1000 times faster than that predicted by the conventional chemistry. The fact that such an extraordinarily strong loss process would have

been overlooked would be a surprise: conventional models not only describe very well the chemistry of methane on Earth, but also reproduce satisfactorily on Mars species that are sensitive to the oxidizing capacity of the atmosphere, such as hydrogen peroxide³², ozone³³ and carbon monoxide³⁴. Unless a mechanism is discovered that can rapidly destroy methane without violating our wide quantitative understanding of Mars photochemistry, all the methane detections reported to date appear incompatible with present TGO measurements.

Methods

The Atmospheric Chemistry Suite (ACS)

ACS¹² consists of three infrared channels featuring high accuracy, high resolving power, and a broad spectral coverage (0.7 to 17 μm). The MIR channel is a high dispersion echelle spectrometer dedicated to solar occultation measurements in the 2.3-4.5 μm range. MIR is conceived to accomplish highly sensitive measurements of the trace gases, while also simultaneously profiling the abundant components, CO_2 , H_2O , and their isotopologues. ACS MIR is a crossed-dispersion spectrometer that measures spectra dispersed onto a cryogenic 512×640 HgCdTe infrared array. For each acquired frame MIR measures up to 20 adjacent diffraction orders, covering an instantaneous spectral range of 0.15-0.3 μm wide. To achieve the full spectral coverage a secondary dispersion grating can be rotated to 11 distinct positions. When tuned to the CH_4 range MIR acquires frames containing 20 adjacent and partially overlapping diffraction orders (172-192) from 3.09 μm to 3.45 μm (see SM F1). The spectral resolving power is $\lambda/\Delta\lambda\approx 50,000$. Together with two other channels [the near-infrared (NIR) and the Fourier-transform spectrometers (TIRVIM)], ACS fully covers the spectral range between 0.7 to 17 μm . NIR and TIRVIM are used to observe (in solar occultation and in nadir) water vapor H_2O , carbon monoxide CO , and other interesting gases including molecular oxygen O_2 . The broad spectral range acquired allows characterization of the atmospheric state: dust loading, and condensation clouds. The temperature profile of the atmosphere is retrieved from the 15- μm CO_2 band measured by TIRVIM in nadir.

The Nadir and Occultation for MArS Discovery (NOMAD)

NOMAD¹⁴ also includes three spectroscopic channels, operating from the ultraviolet (UV) and visible range to 4.3 μm . The channel most sensitive to trace gases is the SO (Solar Occultation, Neefs et al., 2015) spectrometer providing the spectral resolving power of $\lambda/\Delta\lambda\approx 20,000$ in the spectral range of 2.3-4.3 μm . Within this range, NOMAD SO acquires 10 separate wavelength sub-ranges to profile a variety of atmospheric species. The two other channels of NOMAD are the UVIS (Ultraviolet and Visible Spectrometer; 200-650 nm; Patel et al., 2017), and LNO (Limb, Nadir, Occultation) spectrometers that can be operated both in solar occultation and in nadir. NOMAD provides vertical

profiling information for atmospheric constituents at unprecedented spatial and temporal resolution. Indeed, in solar occultation, the vertical resolution is less than 1 km for SO and UVIS, with a sampling rate of 1 s (one measurement every 1 km), and occultations range from the surface to 200 km altitude. NOMAD also provides mapping of several constituents (aerosols/dust/clouds, and O_3 , H_2O , HDO , CO , and other trace gases) in nadir mode with an instantaneous footprint of $0.5 \times 17 \text{ km}^2$ (LNO spectrometer) and 5 km^2 (UVIS spectrometer) respectively, with a repetition rate of 30 Martian days. A more thorough description of the instrument can be found in Neefs et al.² and Patel et al.³. For this work, we analyzed SO channel data measured between April 21st and August 1st. SO measures 4 spectral bins in each of 5 or 6 diffraction orders per second in solar occultation mode, among which a series of specific diffraction orders were chosen (order 133 to 136 spanning 2990 to 3080 cm^{-1} spectral range) where methane features are present.

To increase the sensitivity of the NOMAD SO measurements, we accumulate all the spectral measurements in each occultation from the 4 spectral bins into 3 km vertical bins. The transmittance calibration and error calculation from Trompet et. al. (2016) is adapted to consider this accumulation. By accumulating multiple measurements, we effectively increase the typical 48 ms integration time of a single measurement to an average of 500 ms integration, thereby increasing the SNR.

To estimate a detection limit for each of the resulting NOMAD spectra, we apply a simplified retrieval method described here. The forward model computes the optical column density for each spectrum separately, assuming a constant mixing ratio along the line-of-sight and using the most recent HITRAN CH_4 line list with CO_2 pressure broadening coefficients. The optical depth is then convoluted to the ILS with FWHM of 0.15 cm^{-1} , and then multiplied by the Blaze and AOTF functions.

The chi-squared of the transmittance is fit using the Levenberg-Marquardt algorithm (via the Python Scipy wrapper of MINPACKS lmdr [ref 3]) to determine an optimal polynomial background and CH_4 mixing ratio. The standard error of the mixing ratio is derived from the covariance matrix of the optimal fit parameters. This value can be thought of as the symmetric error bound on the mixing ratio that can affect the transmittance within the measurement noise, and should be a close approximation to the detection limit.

The unconstrained spectral resolution of SAM's laser spectrometer allows for very sensitive detections with the atmospheric sample in the cell of 16.2 meters path length at ambient Mars pressure ($\sim 8 \text{ mbar}$)¹⁷. For a subset of samplings, TLS was operated in a more sensitive mode, where

CO₂, which constitutes 96% of the atmosphere was progressively removed from the sample, enriching the remaining gases by a factor of 25. The achieved accuracy is 1-2 ppbv for the direct intake, and 50-100 pptv for the enrichment mode^{17, 2, 6}. For TGO, the effective optical path during a solar occultation measurement at a slant altitude of xx km is ~300 km; for this geometry, the number of CO₂ molecules along the line of sight (the column density) is $N \approx 10^{24} \text{ cm}^{-2}$. The spectral resolution of the ACS MIR channel is $\sim 0.1 \text{ cm}^{-1}$ (the spectral resolution at which the water line fitting and the profile retrieval, Figure 3, was made). Comparing to $N \approx 3 \cdot 10^{22} \text{ cm}^{-2}$ and the natural, pressure-broadened linewidth of methane $\sim 10^{-2} \text{ cm}^{-1}$ for the case of Curiosity's TLS, one can estimate that the TGO occultation measurements should be theoretically a factor of ~30x more sensitive than what can be achieved with the TLS direct intakes, and of comparable sensitivity to measurements performed in the enrichment mode.

Supplementary material

Figure S1

Figure S2

Figure S3

Potential Referees:

(1) C. Webster, (2) K. Zahnle, (3) R. Zurek, (4), S. Atreya, (5) , G. Piccioni, (6) A. Campargue

Acknowledgments

The NOMAD experiment is led by the Royal Belgian Institute for Space Aeronomy (IASB-BIRA), assisted by Co-PI teams from Spain (IAA-CSIC), Italy (INAF-IAPS), and the United Kingdom (Open University). This project acknowledges funding by the Belgian Science Policy Office (BELSPO), with the financial and contractual coordination by the ESA Prodex Office (PEA 4000103401, 4000121493), by Spanish MICINN through its Plan Nacional and by European funds under grant ESP2015-65064-C2-1-P (MINECO/FEDER), as well as by UK Space Agency through grants ST/R005761/1, ST/P001262/1, ST/R001405/1, and ST/R001405/1 and Italian Space Agency through grant 2018-2-HH.0.

ACS Team

Team +Kokonkov +Savelyeva +Loïc Verdier

L Baggio, G Lacombe

- 1 Space Research Institute (IKI), 84/32 Profsoyuznaya, 117997 Moscow, Russia
- 2 LATMOS/IPSL, UVSQ Université Paris-Saclay, UPMC Univ. Paris 06, CNRS, Guyancourt, France
- 3 LMD CNRS Jussieu, Paris, France
- 4 LATMOS/IPSL, UPMC Univ. Paris 06 Sorbonne Universités, UVSQ, CNRS, Paris, France
- 5 Main Astronomical Observatory MAO NASU, Kyiv, Ukraine
- 6 VNIIFTRI, Mendeleevo, Moscow Region, Russia
- 7 Scientific Production Enterprise Astron Electronics, Orel, Russia
- 8 Physics Department, Lomonosov Moscow State University, Moscow, Russia
- 9 IAPS-INAF, Rome, Italy
- 10 German Aerospace Center DLR, Berlin, Germany
- 11 LESIA, Observatoire de Paris, PSL Research University, CNRS, Sorbonne Universités, UPMC Univ. Paris 06, Univ. Paris Diderot, Sorbonne Paris Cité, Paris, France
- 13 Max-Planck-Institut für Sonnensystemforschung, Göttingen, Germany
- 14 Tohoku University, Sendai, Miyagi, Japan
- 15 Moscow Institute of Physics and Technology (MIPT), Dolgoprudny, Moscow Region, Russia
- 16 Catholic University, Washington DC, USA
- 17 Vernadsky Institute of Geochemistry and Analytical Chemistry GEOKHI, Moscow, Russia
- 18 Instituto de Astrofísica de Andalucía/CSIC, Granada, Spain
- 19 Department of Computer Science, Luleå University of Technology, Kiruna, Sweden
- 20 Instituto Andaluz de Ciencias de la Tierra (CSIC-UGR), Granada, Spain
- 21 Open University, Milton-Keynes, UK
- 22 Laboratoire de Géologie de Lyon, Université Lyon, Lyon, France
- 23 Institute of Astronomy RAS, Moscow, Russia
- 24 Royal Belgium Institute of Aeronomy BIRA/IASB, Brussels, Belgium
- 25 University of Bern, Bern, Switzerland
- 26 Facultad de Informatica, Universidad Complutense de Madrid, Madrid, Spain
- 27 Institut d'Astrophysique Spatiale IAS, CNRS/Université Paris Sud, Orsay, France
- 28 Physics Department, Oxford University, Oxford, UK

References

1. Mumma, M. J. et al. Strong Release of Methane on Mars in Northern Summer 2003. *Science* **323**, 1041-1045, doi:10.1126/science.1165243 (2009).
2. Webster, C. R. et al. Mars methane detection and variability at Gale crater. *Science* **347**, 415-417 (2015).
3. Krasnopolsky, V. A., Maillard, J. P. & Owen, T. C. Detection of methane in the martian atmosphere: evidence for life? *Icarus* **172**, 537-547 (2004).
4. Krasnopolsky, V. Search for methane and upper limits to ethane and SO₂ on Mars. *Icarus* **217**, 144-152, doi:10.1016/j.icarus.2011.10.019 (2012).
5. Villanueva, G. L. et al. A sensitive search for organics (CH₄, CH₃OH, H₂CO, C₂H₆, C₂H₂, C₂H₄), hydroperoxyl (HO₂), nitrogen compounds (N₂O, NH₃, HCN) and chlorine species (HCl, CH₃Cl) on Mars using ground-based high-resolution infrared spectroscopy. *Icarus* **223**, 11-27 (2013).
6. Webster, C. R. et al. Background levels of methane in Mars' atmosphere show strong seasonal variations. *Science* **360**, 1093-1096 (2018).
7. Lefèvre, F. & Forget, F. Observed variations of methane on Mars unexplained by known atmospheric chemistry and physics. *Nature* **460**, 720-723 (2009).
8. Formisano, V., Atreya, S., Encrenaz, T., Ignatiev, N. & Giuranna, M. Detection of Methane in the Atmosphere of Mars. *Science* **306**, 1758-1761 (2004).
9. Geminale, A., Formisano, V. & Sindoni, G. Mapping methane in Martian atmosphere with PFS-MEX data. *Planet. Space Sci.* **59**, 137-148, doi:10.1016/j.pss.2010.07.011 (2011).
10. Zurek, R. W. et al. Assessment of a 2016 mission concept: The search for trace gases in the atmosphere of Mars. *Planet. Space Sci.* **59**, 284-291, doi:10.1016/j.pss.2010.07.007 (2011).
11. Vago, J. et al. ESA ExoMars program: The next step in exploring Mars. *Solar System Research* **49**, 518-528 (2015).
12. Svedhem, H., Vago, J. L., Mutschdörfer, P., de Groot, R., Montagna, M., Renaud, P.-Y.: 2018, The ExoMars Trace Gas Orbiter, *Space Sci. Rev.* **214**. In press (2018).
13. Korablev, O. et al. The Atmospheric Chemistry Suite (ACS) of three spectrometers for the ExoMars 2016 Trace Gas Orbiter. *Space Sci. Rev.* **214:7**, doi:10.1007/s11214-11017-10437-11216 (2018).
14. Vandaele, A. C. et al. NOMAD, an integrated suite of three spectrometers for the ExoMars Trace Gas mission: technical description, science objectives and expected performance. *Space Sci. Rev.* **214:80**, doi:10.1007/s11214-018-0517-2 (2018).

15. Vandaele, A. C. et al. This issue (2018).
16. Fedorova, A. et al. Water vapor in the middle atmosphere of Mars during the 2007 global dust storm. *Icarus* **300**, 440-457, doi:10.1016/j.icarus.2017.09.025 (2018).
17. Webster, C. R. et al. Low Upper Limit to Methane Abundance on Mars. *Science* **342**, 355-357 (2013).
18. Atreya, S., Mahaffy, P. & Wong, A. Methane and related trace species on Mars: Origin, loss, implications for life, and habitability. *Planet. Space Sci.* **55**, 358-369, doi:10.1016/j.pss.2006.02.005 | 10.1016/j.pss.2006.02.005 (2007).
19. Etiope, G. & Sherwood Lollar, B. Abiotic Methane on Earth. *Reviews of Geophysics* **51**, 276-299 (2013).
20. Oehler D. & Etiope G. Methane seepage on Mars: where to look and why. *Astrobiology* **17**, 1233-1264 (2017).
21. Etiope, G., Oehler, D. Z. & Allen, C. C. Methane emissions from Earth's degassing: Implications for Mars. *Planet. Space Sci.* **59**, 182-195 (2011).
22. Etiope G., Ehlmann B. & Schoell M. Low-temperature production and exhalation of methane from serpentinized rocks on Earth: a potential analog for methane production on Mars. *Icarus* **224**, 276-285 (2013).
23. Max, M.D., Clifford, S.M. & Johnson, A.H. Hydrocarbon system analysis for methane hydrate exploration on Mars. *Amer. Assoc. Petrol. Geol. Memoir* **101**, 99-114 (2013).
24. Etiope G. & Martinelli G. Migration of carrier and trace gases in the geosphere: an overview. *Phys. Earth Planet. Int.* **129**, 3-4, 185-204 (2002).
25. Meslin, P. Y., Gough, R., Lefèvre, F. & Forget, F. Little variability of methane on Mars induced by adsorption in the regolith. *Planet. Space Sci.* **59**, 247-258, doi:10.1016/j.pss.2010.09.022 (2011).
26. Trainer, M. G., Tolbert, M. A., McKay, C. P. & Toon, O. B. Limits on the trapping of atmospheric CH₄ in martian polar ice analogs. *Icarus* **208**, 192-197 (2010).
27. Mischna, M. A., Allen, M., Richardson, M. I., Newman, C. E. & Toigo, A. D. Atmospheric modeling of Mars methane surface releases. *Planetary and Space Science* **59**, 227-237, doi:10.1016/j.pss.2010.07.005 (2011).
28. Viscardi, S., Daerden, F. & Neary, L. Formation of layers of methane in the atmosphere of Mars after surface release. *Geophysical Research Letters* **43**, 1868-1875 (2016).
29. Knapmeyer, M. et al. Working models for spatial distribution and level of Mars' seismicity. *Journal of Geophysical Research (Planets)* **111**, E11006 (2006).

30. Tyler, D. & Barnes, J. R. Convergent crater circulations on Mars: Influence on the surface pressure cycle and the depth of the convective boundary layer. *Geophysical Research Letters* 42, 7343-7350 (2015).
 31. Vasavada, A. R. et al. Assessment of Environments for Mars Science Laboratory Entry, Descent, and Surface Operations. *Space Science Reviews* 170, 793-835 (2012).
 32. Encrenaz, T. et al. Seasonal variations of hydrogen peroxide and water vapor on Mars: Further indications of heterogeneous chemistry. *Astronomy & Astrophysics* 578, A127. <https://doi.org/10.1051/0004-6361/201425448> (2015).
 33. Clancy, R. T. et al.. (2016). Daily global mapping of Mars ozone column abundances with MARCI UV band imaging. *Icarus* 266, 112–133. <https://doi.org/10.1016/j.icarus.2015.11.016> (2016).
 34. Smith, M.D. et al. The climatology of carbon monoxide and water vapor on Mars as observed by CRISM and modeled by the GEM-Mars general circulation model. *Icarus* 301, 117–131. <https://doi.org/10.1016/j.icarus.2017.09.027> (2018).
-
- Neefs, E. et al. NOMAD spectrometer on the ExoMars trace gas orbiter mission: part 1—design, manufacturing, and testing of the infrared channels. *Applied Optics* 54, 8494-8520, doi:<http://dx.doi.org/10.1364/AO.54.008494> (2015).
- Patel, M. R. et al. The NOMAD spectrometer on the ExoMars Trace Gas Orbiter mission: part 2—design, manufacturing, and testing of the ultraviolet and visible channel. *Applied Optics* 56, 2771-2782, doi:<https://doi.org/10.1364/AO.56.002771> (2017).
- Neary, L. & Daerden, F. The GEM-Mars General Circulation Model for Mars: Description and Evaluation. *Icarus* 300, 458–476, doi:<https://doi.org/10.1016/j.icarus.2017.09.028> (2018).
-